Journal of Catalysis 287 (2012) 210–213

Contents lists available at SciVerse ScienceDirect

Journal of Catalysis

journal homepage: www.elsevier.com/locate/jcat

Letter to the Editor

Comment on "Towards understanding the bifunctional hydrodeoxygenation and aqueous phase reforming of glycerol" [J. Catal. 269 (2010) 411–420]

ARTICLE INFO

Article history:
Available online 9 January 2012

Keywords:
Dehydrogenation
Propanol
Propanal
Acetone
Aqueous phase reforming
DFT calculations

ABSTRACT

A recent experimental study of 1- and 2-propanol in water feed over Pt/Al_2O_3 yielded dehydrogenation of 2-propanol to acetone, but formation of CO_2 and ethane from 1-propanol. To rationalize this reactivity difference of primary and secondary alcohols, we explored computationally the dehydrogenation of 1- and 2-propanol over Pt(111) as model. As product of 2-propanol, our calculations confirm acetone which adsorbs only weakly; thus, desorption occurs readily as the subsequent dehydrogenation would exhibit a high barrier. For 1-propanol we determined propionyl as strongly adsorbed intermediate which eventually undergoes C-C bond breaking.

1. Introduction

The heterogeneous catalysis of alcohols over transition metal catalysts comprises complex reaction networks which include oxygenated species as intermediates [1]. Understanding the selective conversion of such oxygenated species is of particular interest for an efficient production of hydrogen and chemicals from biomass feedstocks via aqueous phase processing [2,3].

The chemistry of alcohols over transition metal surfaces has extensively been studied [4,5]. Accordingly, a generally applicable sequence of reactions is taking place when alcohols are adsorbed on transition metal surfaces. This sequence starts with an abstraction of the hydroxyl hydrogen, followed by H elimination from the resulting alkoxide carbon. Subsequent dehydrogenation steps yield carbonyl and acyl species [1].

Recently, Wawrzetz et al. [6] explored the scission of C-C and C-O bonds of glycerol in water over Pt/Al_2O_3. In a density functional theory (DFT) study, Coll et al. [7] explored the intermediates formed by dehydration and subsequent hydrogenation of glycerol, a mechanism listed by the experimentalists as a possible route of reforming [6]. Yet, based on batch experiments on the simple alcohols 1- and 2-propanol, the experimentalists favored an alternative pathway [6] that starts with dehydrogenation. Over Pt/Al_2O_3 catalyst, they found 1-propanol to behave differently from 2-propanol under identical conditions (at 473 K under 20 bar total pressure with a feed of 10 wt.% propanol over Pt particles of 1.5 nm average size in the absence of hydrogen) [6]. While for 2-propanol, mainly acetone was observed along with half as much propane as product, for 1-propanol in the first hour mainly propanal was detected, and at the end of the experiments, after five hours, ethane and CO_2 were the main products with a small amount of propionic acid present. Wawrzetz et al. [6] concluded that the small amount of propane was produced via dehydration on the alumina support. As for 2-propanol only dehydrogenation occurs on the metal surface, we carried out a computational study to examine the different behavior of 1- and 2-propanol along the dehydrogenation route over Pt(111) as model catalyst. For that purpose we applied a plane-wave-based DFT method to periodic slab models; computational details are provided as Supporting Data (SD).

2. Results and discussion

We examined computationally four consecutive dehydrogenation steps for 1-propanol (**1a**) and three such reactions for 2-propanol (**2a**). In the latter case, the intermediate to react in the third step is weakly bound and will desorb instead of passing over the high barrier; hence we did not study the fourth step of the chain starting with **2a**. For corresponding reactions among the first three steps of the two reaction chains, we will discuss similarities and differences between initial states (IS) and final states (FS), as well as the transition states (TS), addressing geometries and energetics. The intermediates calculated as stable species on the surface are sketched in Fig. 1 together with pertinent distances and binding energies (BEs). The corresponding TS structures are collected in Fig. 2. In the FS structures, hydrogen is co-adsorbed with the dehydrogenated species; before the next step, this dissociated hydrogen is assumed to diffuse to a distant location. Fig. 3 compares thermodynamic and kinetic characteristics of the two reaction chains.

2.1. Dehydrogenation of the alcohol

We considered the adsorption of **1a** and **2a** in η^1(O) configurations (Fig. 1), mediated via an oxygen lone pair. This type of complex was discussed as the most stable structure for various alcohols

0021-9517/$ - see front matter © 2011 Elsevier Inc. All rights reserved.
doi:10.1016/j.jcat.2011.12.010

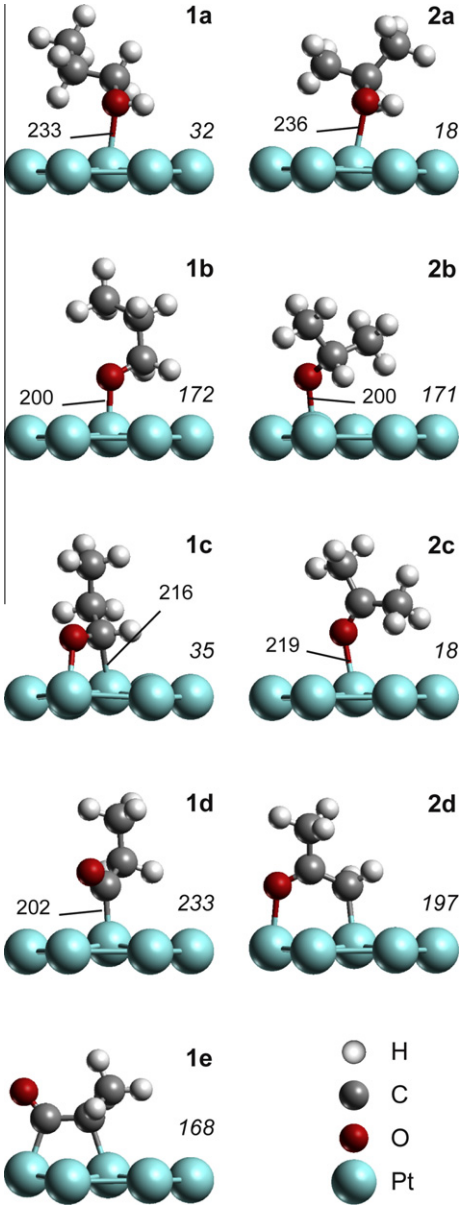

Fig. 1. Optimized structures of 1- and 2-propanol and their dehydrogenation products on Pt(1 1 1): **1a** – 1-propanol, **1b** – 1-propoxy, **1c** – propanal, **1d** – propionyl, **1e** – methylketene, **2a** – 2-propanol, **2b** – 2-propoxy, **2c** – acetone, **2d** – 2-oxopropyl. Numbers in italics indicate calculated BEs (kJ mol^{-1}). Selected distances (pm) are also shown.

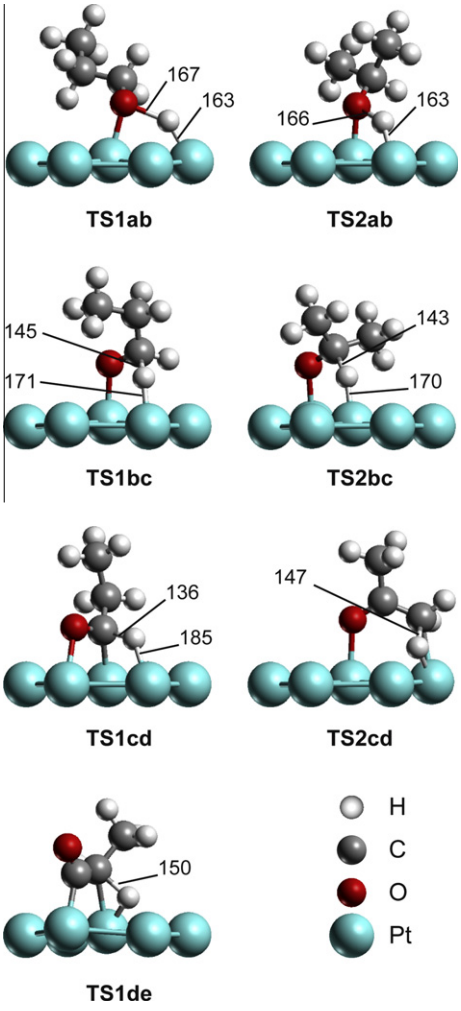

Fig. 2. Structures of transition states TSnxy of various dehydrogenation steps of 1- and 2-propanol on Pt(1 1 1). Structure TSnxy characterizes the conversion of compound **nx** to compound **ny** as given in Fig. 1. Selected distances (pm) are also shown.

on transition metal surfaces [1,5]. The BE values of these species are low, 32 kJ mol^{-1} for **1a** and 18 kJ mol^{-1} for **2a** (Fig. 1), suggesting a quasi-equilibrium between adsorption and desorption processes. The calculated BE of **2a** is close to the experimental value [8], 24 kJ mol^{-1}, estimated from temperature programmed desorption for **2a** adsorbed on a Pt catalyst supported by activated carbon. That experimental energy is also very close to our estimate for the primary alcohol **1a**.

In the calculated structures **1a** and **2a**, the hydroxyl hydrogen to be eliminated points toward the surface (Fig. 1). This H atom will form a bond with a neighboring Pt atom. In **TS1ab** for 1-propanol and **TS2ab** for 2-propanol, the distance H–Pt = 163 pm is rather short. The H–O bond elongates to the same extent in both alcohols (Fig. 2). As the reaction is endothermic, the TS is expected to be late which indeed is corroborated by shortened H–Pt and elongated H–O bonds. The reaction energies were calculated at 45 kJ mol^{-1} for the primary and 39 kJ mol^{-1} for the secondary alcohol. The corresponding barriers are also very similar, 62 kJ mol^{-1} for 1-propanol and 58 kJ mol^{-1} for 2-propanol. In a DFT study [9], Alcalá et al. calculated qualitatively similar reaction energies (1-propanol: 58 kJ mol^{-1}, 2-propanol: 53 kJ mol^{-1}) and barriers (77 and 71 kJ mol^{-1}, respectively). Rioux and Vannice [8] estimated the activation energies of 2-propanol dehydrogenation as 38–48 kJ mol^{-1} when catalyzed by Pt powder of ultra-high purity and as 28–30 kJ mol^{-1} when catalyzed by Pt supported on activated carbon.

In view of their radical structures (in the gas phase), it is no surprise that the resulting alkoxides, 1-propoxy (**1b**) and 2-propoxy (**2b**), bind strongly, 171–172 kJ mol^{-1}, to the surface through the dehydrogenated oxygen center – much stronger than their (closed-shell) hydrogenated counterparts **1a** and **2a** (Fig. 1). In consequence, both species get 30 pm closer to the adsorption site; the C–O bonds shorten by ~6 pm.

2.2. Dehydrogenation of the alkoxide

The next step in the decomposition of the alcohols is the abstraction of a hydrogen geminal to the O center to form a carbonyl: propanal (**1c**) from 1-propoxy (**1b**), acetone (**2c**) from 2-propoxy (**2b**, Fig. 1). Once again, the transition states of the two dehydrogenating species are very similar, both structurally and energetically. The dissociating H atom (initially C–H ≈ 113 pm)

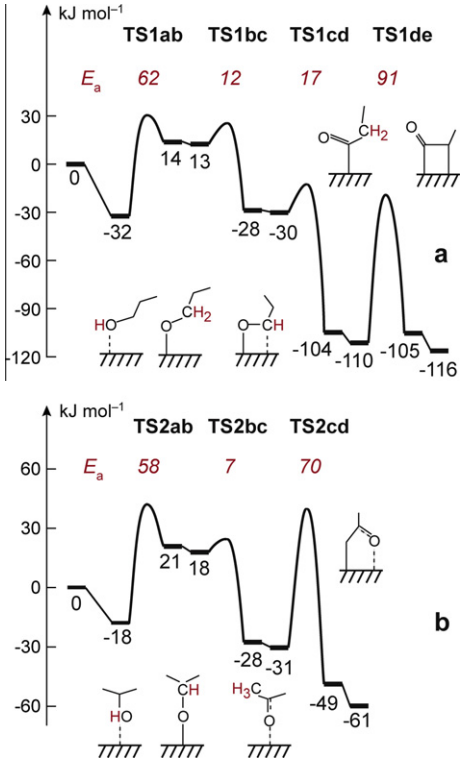

Fig. 3. Calculated energy profiles of alcohol dehydrogenation on Pt(1 1 1) at coverage 1/9: comparison of analogous steps for (a) 1-propanol and (b) 2-propanol. Reaction energies are referenced to the corresponding alcohol molecule in the gas phase and the clean surface. Structures with hydrogen co-adsorbed after C–H scission and the same C3 species in the initial state of the subsequent dehydrogenation step differ by the interaction energy of the co-adsorbed species, C3 and H, which is assumed to be released by the diffusion of hydrogen to "infinite" separation. Arcs represent reaction barriers of the various dehydrogenation steps; the corresponding activation energies are listed as E_a values (in italics). All energies in kJ mol^{-1}.

interacts with the nearest Pt atom, approaching a top position in the TS (**TS1bc**, **TS2bc**; Fig. 2) with C–H = 143–145 pm and a newly formed H–Pt ≈ 171 pm. This second dehydrogenation step is exothermic, releasing 42 kJ mol^{-1} and 46 kJ mol^{-1} for 1-propoxy and 2-propoxy, respectively (Fig. 3). The corresponding barriers are extremely low, only 12 and 7 kJ mol^{-1}, respectively. These values point to a very fast conversion, rendering the detection of propoxy species on the surface difficult.

After this second dehydrogenation step, the decomposition networks of 1- and 2-propanol begin to differ in an essential way, in their most stable product complexes. In the FS of the chain starting from 1-propanol, propanal adsorbs in η^2 fashion, with the carbonyl moiety oriented parallel to the surface (**1c**, Fig. 1). This structure is 13 kJ mol^{-1} more stable than its η^1 counterpart where the carbonyl moiety is oriented upright relative to the surface (not shown). In contrast, in the FS of the chain starting from 2-propanol, the η^1 mode of acetone (**2c**, Fig. 1) is calculated 14 kJ mol^{-1} more stable than the corresponding η^2 complex (not shown) where the methyl groups would undergo a repulsive interaction with the surface. At variance with our result, Alcalá et al. [9] and Khanra et al. [10] used the η^1 mode when calculating the hydrogenation of propanal on Pt(1 1 1). Our result for acetone, i.e., preferential adsorption in η^1 fashion on Pt(1 1 1), agrees with previous experimental [11–13] and theoretical studies [9,14].

2.3. Dehydrogenation of the carbonyl

Thus far, the TSs of both reaction chains were structurally and energetically very similar. However, the products of the second dehydrogenation, propanal (**1c**) and acetone (**2c**), adsorb in different modes; therefore, one anticipates that the TSs of the subsequent conversion steps will also differ. Also, calculations on species in the gas phase show a C–H bond of acetone to be 30 kJ mol^{-1} stronger than the C–H bond that is broken in propanal.

In the dehydrogenation of the η^2 adsorption complex **1c**, the hydrogen ligand at the carbon center bound to the surface will interact with a Pt atom. In the resulting transition state **TS1cd** (Fig. 2), C–H = 136 pm and H–Pt = 185 pm. This dehydrogenation process is exothermic by 74 kJ mol^{-1} over a barrier of only 17 kJ mol^{-1}, forming propionyl (**1d**, Fig. 1) which, being a radical, strongly binds to the surface (in η^1 fashion).

In contrast, the dehydrogenation of acetone **2c** involves a hydrogen atom of a methyl group. In the corresponding structure **TS2cd** (Fig. 2), acetone forms an oxametallacycle with surface atoms and the leaving hydrogen binds at the same Pt atom to which the CH_2 group attaches (C–H = 147 pm, the newly formed H–Pt = 175 pm). This TS structure is very close to that of the FS **2d** (Fig. 1), also an oxametallacycle. The dehydrogenation of acetone is also exothermic, but by 18 kJ mol^{-1} only, and the corresponding barrier, 70 kJ mol^{-1}, is much higher than that for the conversion of propanal (Fig. 3). As the activation energy of acetone (**2c**) to form 2-oxopropyl (**2d**) is calculated much higher than its BE, 18 kJ mol^{-1}, one expects the surface species **2c** to desorb rather than to dehydrogenate.

For these decisive third steps, we also considered solvent effects; see SD. We optimized two models for each of the alcohol derived molecules: (*i*) close to the surface, covered by a water layer, to represent the adsorbed mode and (*ii*) over a water layer on the surface to approximate the desorbed mode. In the structure resulting for acetone adsorbed on the surface (see SD, Fig. S1, **2c-ads**), the O center is more than 400 pm from the metal surface, indicating a transfer into the aqueous phase without any barrier. In fact, it is even more favorable, by 47 kJ mol^{-1}, to place acetone above the water layer (Fig. S1, **2c-des**). The adsorbed structure of propanal (Fig. S1, **1c-ads**) is stabilized on the surface with bond lengths of C–Pt = 217 pm and O–Pt = 209 pm. The C–O bond of this adsorbed species is 140 pm (Fig. S1, **1c-ads**), while it shrinks to 125 pm when stabilized over the water layer (Fig. S1, **1c-des**). The latter structure, **1c-des**, with propanal over the water layer is by 59 kJ mol^{-1} more stable than the system with propanal adsorbed directly at the surface, **1c-ads**. However, upon transfer into the solvent, propanal changes its structure to that in the adsorption complex **1c-ads**, requiring 160 kJ mol^{-1} if carried out in the gas phase. Thus, if propanal left the surface with its structure fixed as in **1c-ads**, its shape would be strongly unfavorable, even in solution. This implies a relaxation due to solvation and, likely, a barrier of this transfer reaction. To examine this transfer in more detail, we calculated the corresponding energy change for the solute at various heights above the surface, for both the adsorbed structure ("inner sphere") and the structure above the solvent ("outer sphere"); see SD, Fig. S2. Moving the solute at fixed adsorbate structure upward and the desorbed solute at fixed geometry down into the solvent, one calculates energy curves that intersect at energies above the adsorption complex, ~190 kJ mol^{-1} for **1c** and ~14 kJ mol^{-1} for **2c**. Relaxing these intermediate geometries decreases the energy by about the solvation energy, 160 kJ mol^{-1} for propanal, but only 2 kJ mol^{-1} for acetone. These results suggest an activation barrier in the case of propanal, even after accounting for this relaxation. Indeed, the simple solvation model for propanal leaving the surface features a TS with an activation barrier of 28 kJ mol^{-1} (see SD, Fig. S3), in good agreement with the estimated energy gain due to solvation.

Hence, the simple solvation models support the desorption of acetone, but suggest for propanal the possibility of further dehydrogenation. Indeed, Wawrzetz et al. [6] observed acetone as the

major product in the conversion of 2-propanol over Pt/γ-Al_2O_3. Rioux and Vannice [8] reported 100% selectivity to acetone compared to propylene for Pt supported on activated carbon.

2.4. Dehydrogenation of propionyl

In view of the above, we restricted the fourth dehydrogenation step to the oxygenate propionyl (**1d**), derived from 1-propanol (**1a**). In this step, a hydrogen at the α-carbon center is removed to form methyl ketene (**1e**, Fig. 1). In the transition state **TS1de** (Fig. 2), the leaving H is almost at a Pt–Pt bridge position, and the corresponding C atom begins to form a bond to the Pt atom with which the leaving H initially interacted. Thus, this structure bears some similarity to that of **TS2cd** of acetone. The reaction **1d** → **1e** is endothermic by 4 kJ mol^{-1} only, i.e., essentially thermoneutral. The corresponding barrier, 91 kJ mol^{-1} (Fig. 3a), is the highest calculated among all reactions in this study. Thus, conversion of propionyl to methyl ketene is difficult. Propionyl (**1d**) is calculated to adsorb strongly on Pt(1 1 1) with BE = 233 kJ mol^{-1}. Therefore, in contrast to acetone (**2c**), one does not expect propionyl to desorb under the experimental conditions reported by Wawrzetz et al. [6].

3. Conclusions

In this work, we explored computationally the dissimilar reactivity patterns observed when 1- and 2-propanol are converted under the same experimental conditions [6]. For this purpose, we focused on dehydrogenation processes because for 2-propanol these apparently are the only transformations taking place.

In a phenomenological fashion, one is able to rationalize the unequal reaction patterns of 1- and 2-propanol [6] by considering the activation energies calculated for a (potential) third dehydrogenation step in the two reaction chains (Fig. 3). Obviously, propanal (**1c**) is easily dehydrogenated to adsorbed propionyl (**1d**), over a small barrier of only 17 kJ mol^{-1}. In fact, it should be possible to identify propionyl (**1d**) on the metal surface where it binds quite strongly (Fig. 1). In contrast, in a third, essentially thermoneutral dehydrogenation step, acetone (**2c**) would have to overcome a rather high barrier of 70 kJ mol^{-1} to dehydrogenate the α-hydrogen to form 2-oxopropyl (**2d**) over Pt. Instead, the weakly adsorbed acetone desorbs from the surface, moving into the aqueous phase, as found in experiment [6]. Models with an approximate representation of the aqueous phase for propanal and acetone corroborated this rationalization.

These substantially different reactivity patterns of the two types of oxygenates, propanal (**1c**) and acetone (**2c**), can be rationalized in a more fundamental way. First, note that the structures of the intermediates **1c** and **2c** after two consecutive dehydrogenation steps differ notably (Fig. 1). Propanal (**1c**) is calculated to adsorb with its carbonyl moiety essentially parallel to the surface, hardly requiring rearrangement when the C–H bond is cleaved. On the other hand, in the adsorption complex of acetone (**2c**) the carbonyl group is oriented essentially perpendicular to the metal surface. In consequence, an additional energy of 14 kJ mol^{-1} is required to reach an orientation favorable for the next dehydrogenation step. Second, as estimated for species in the gas phase, C–H bonds of acetone are 30 kJ mol^{-1} stronger than the C–H bond of the carbonyl moiety of propanal **1c**.

Acknowledgments

The authors thank Prof. J. A. Lercher for stimulating discussions. DB is grateful for a fellowship of the European Graduate School of Sustainable Energy Technologies. This work was supported by Fonds der Chemischen Industrie (Germany) and generous computing resources at Leibniz Rechenzentrum München.

Appendix A. Supporting data

Supplementary data associated with this article can be found, in the online version, at doi:10.1016/j.jcat.2011.12.010.

References

[1] M. Mavrikakis, M.A. Barteau, J. Mol. Catal. A: Chem. 131 (1998) 135–147.
[2] R.D. Cortright, R.R. Davda, J.A. Dumesic, Nature 418 (2002) 964–967.
[3] G.W. Huber, R.D. Cortright, J.A. Dumesic, Angew. Chem. Int. Ed. 43 (2004) 1549–1551.
[4] M.A. Vannice, W. Erley, H. Ibach, Surf. Sci. 254 (1991) 12–20.
[5] L.J. Shorthouse, A.J. Roberts, R. Raval, Surf. Sci. 480 (2001) 37–46.
[6] A. Wawrzetz, B. Peng, A. Hrabar, A. Jentys, A.A. Lemonidou, J.A. Lercher, J. Catal. 269 (2010) 411–420.
[7] D. Coll, F. Delbecq, Y. Array, P. Sautet, Phys. Chem. Chem. Phys. 13 (2011) 1448–1459.
[8] R.M. Rioux, M.A. Vannice, J. Catal. 233 (2005) 147–165.
[9] R. Alcalá, J. Greeley, M. Mavrikakis, J.A. Dumesic, J. Chem. Phys. 116 (2002) 8973–8980.
[10] B.C. Khanra, Y. Jugnet, J.C. Bertolini, J. Mol. Catal. A: Chem. 208 (2004) 167–174.
[11] N.R. Avery, Surf. Sci. 125 (1983) 771–786.
[12] N.R. Avery, W.H. Weinberg, A.B. Anton, B.H. Toby, Phys. Rev. Lett. 51 (1983) 682.
[13] M.A. Vannice, W. Erley, H. Ibach, Surf. Sci. 254 (1991) 1–11.
[14] E.L. Jeffery, R.K. Mann, G.J. Hutchings, S.H. Taylor, D.J. Willock, Catal. Today 105 (2005) 85–92.

Duygu Basaran
Alexander Genest
Notker Rösch
Department Chemie and Catalysis Research Center, Technische Universität München, 85747 Garching, Germany
E-mail address: roesch@mytum.de (N. Rösch)